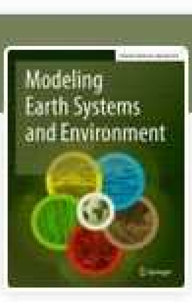

Modeling Earth Systems and Environment

Editorial board
Aims & scope

The peer-reviewed journal *Modeling Earth Systems and Environment* (MESE) provides a unique publication platform by discussing interdisciplinary problems and approaches through modeling. The focus of MESE is on modeling in earth and environment related fields, such as: earth and environmental engineering; climate change; hydrogeology; aquatic systems and functions; atmospheric research and water; land use and vegetation change; modeling of forest and agricultural dynamics; and economic and energy systems. Furthermore, the journal combines these topics with modeling of anthropogenic or social phenomena and projections to be used by decision makers. — show all

Publishing model
Hybrid (Transformative Journal). How to publish with us, including Open Access

31 days
Submission to first decision

342,488 (2021)
Downloads

You have access to our articles

For authors

Submission guidelines
Ethics & disclosures
Open Access fees and funding
Contact the journal
Submit manuscript

Explore

Online first articles
Volumes and issues
Collections
Sign up for alerts

Latest issue

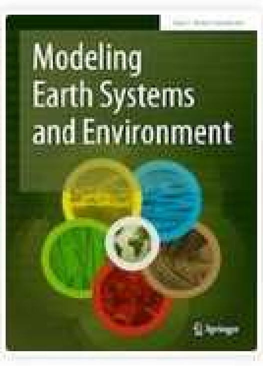

Volume 7
Issue 4, November 2021

View all volumes and issues

Latest articles

Modeling of magnitude and frequency of extreme rainfall in Somalia

Jama Mohamed & Mohd Bakri Adam
Original Article | Published: 24 February 2022

Association between forecasting models' precision and nonlinear patterns of daily river flow time series

Farhang Rahmani & Mohammad Hadi Fattahi
Original Article | Published: 24 February 2022

Impact of wind speed on optimal fishing effort

Ali Labriji, Youssef El Foutayeni & Mostafa Rachik
Original Article | Published: 21 February 2022

Artificial neural networks vis-à-vis MODFLOW in the simulation of groundwater: a review

Nejat Zeydalinejad
Review Article | Published: 21 February 2022

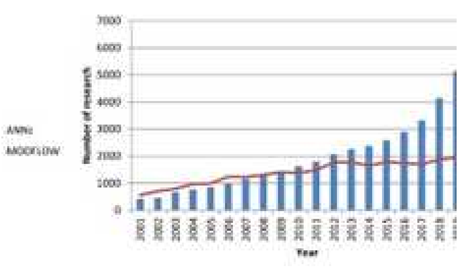

Saint–Venant equations simulation by finite volume method and ULTIMATE strategy

Seyedreza Hashemineiad & Wuyi Wan
Original Article | Published: 21 February 2022

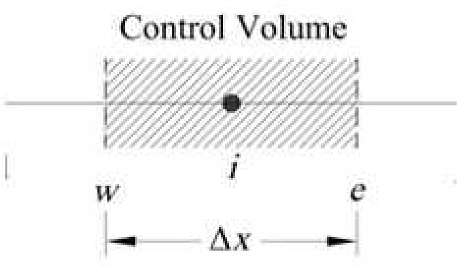

This journal has 41 open access articles

View all articles

About this journal

Electronic ISSN 2363-6211
Print ISSN 2363-6203

Abstracted and indexed in
CLOCKSS
CNKI
CNPIEC
Dimensions
EBSCO Discovery Service
Emerging Sources Citation Index
GeoRef
Google Scholar
Japanese Science and Technology Agency (JST)
Naver
Norwegian Register for Scientific Journals and Series
OCLC WorldCat Discovery Service
Portico
ProQuest Aquatic Sciences and Fisheries Abstracts (ASFA)
ProQuest-ExLibris Primo
ProQuest-ExLibris Summon
SCImago
SCOPUS
Semantic Scholar
TD Net Discovery Service

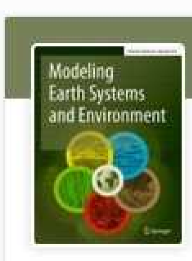

Modeling Earth Systems and Environment

Editors

Modeling Earth Systems and Environment

For authors

Submission guidelines
Ethics & disclosures
Open Access fees and funding
Contact the journal
Submit manuscript

Explore

Online first articles
Volumes and issues
Collections
Sign up for alerts

Volume 7, issue 1, March 2021

51 articles in this issue

Modeling and investigating the effect of the LID methods on collection network of urban runoff using the SWMM model (case study: Shahrekord City)
Majid Omidi Arjenaki, Hamed Reza Zarif Sanayei ... Niloofar Aghili Mahabadi
Review Article | Published: 30 June 2020 | Pages: 1 - 16

Modeling of rainfall variability using functional principal component method: a case study of Taiz region, Yemen
Mohanned Abduljabbar Hael
Original Article | Published: 09 July 2020 | Pages: 17 - 27

Mathematical modeling and a month ahead forecast of the coronavirus disease 2019 (COVID-19) pandemic: an Indian scenario
Suhail Ganiny & Owais Nisar
Original Article | Published: 19 January 2021 | Pages: 29 - 40

Modeling the natural regeneration of *Cedrus libani* A. Richard in Slenfeh, Syria, using binary logistic regression
Abeer Ibrahem, Emad Koubaily & Ali Thabeet
Original Article | Published: 01 September 2020 | Pages: 41 - 55

Modelling historic and future land use/land cover changes and their impact on wetland area in Shashe sub-catchment, Zimbabwe
Sethi Sibanda & Fethi Ahmed
Original Article | Published: 17 September 2020 | Pages: 57 - 70

Modeling on approximation of fluvial landform change impact on morphodynamics at Madhumati River Basin in Bangladesh
Rathindra Nath Biswas, Md. Nazrul Islam ... Sanjib Sarker Shawon
Original Article | Published: 20 October 2020 | Pages: 71 - 93

Modelling the trends of resistivity gradient in hydrogeological units: a case study of alluvial environment
N. Jimmy George
Original Article | Published: 02 November 2020 | Pages: 95 - 104

Climate change and distribution of zoonotic cutaneous leishmaniasis (ZCL) reservoir and vector species in central Iraq
[illegible]

Direct current electrical resistivity forward modeling using comsol multiphysics
[illegible]

Soil erosion modeling using GIS and revised universal soil loss equation approach: a case study of Guna-Tana landscape, Northern Ethiopia
[illegible]

Spatiotemporal analysis of meteorological drought in a Mediterranean dry land: case of the Cheliff basin–Algeria
[illegible]

Groundwater potential evaluation using geoelectrical and analytical hierarchy process modeling techniques in Akure-Owode, southwestern Nigeria
[illegible]

Application of fuzzy expert decision-making system for rock slope block-toppling modeling and assessment: a case study
[illegible]

Tree suitability modeling and mapping in Nepal: a geospatial approach to scaling agroforestry
[illegible]

Time-series analysis of cow milk production at Andassa dairy farm, West Gojam Zone, Amhara Region, Ethiopia
[illegible]

Landslide hazard risk modeling in north-west of Iran using optimized machine learning models
Ali Jamali
Original Article | Published: 30 June 2020 | Pages: 191 - 208

A comprehensive study of different feature selection methods and machine-learning techniques for SODAR structure classification
Nishant Kumar, Kirti Soni & Ravinder Agarwal
Original Article | Published: 09 July 2020 | Pages: 209 - 220

Land deformation monitoring using optical remote sensing and PS-InSAR technique nearby Gangotri glacier in higher Himalayas
Harikesh Singh & A. C. Pandey
Original Article | Published: 19 July 2020 | Pages: 221 - 233

Statistical analysis of high-resolution mesoscale meteorology derived from weather research and forecasting model
Awkash Kumar, Shraddha Dhakhwa & Mayank Kumar
Original Article | Published: 22 July 2020 | Pages: 235 - 245

Investigating the impact of injection-water salinity and well strategies on water mobility and oil production in an oil-wet reservoir
Muhammad Jawad Khan, Temoor Muther ... Muhammad Mubeen-ur-Rehman
Original Article | Published: 16 August 2020 | Pages: 247 - 260

Comparison of trends in apparent and air temperature for climate change assessment
C. Sivapragasam & N. Natarajan
Original Article | Published: 11 October 2020 | Pages: 261 - 271

Soil erosion risk and sediment yield assessment with universal soil loss equation and GIS: in Dijo watershed, Rift valley Basin of Ethiopia
Bagegnehu Bekele & Yenealem Gemi
Original Article | Open Access | Published: 10 November 2020 | Pages: 273 - 291

Stratigraphic modeling and hydraulic characterization of a typical basaltic aquifer system in the Kadva river basin, Nashik, India
Nitin Rane & Geetha K. Jayaraj
Original Article | Published: 20 October 2020 | Pages: 293 - 306

Assessing the influence of climate model biases in predicting yield and irrigation requirement of cassava
Raji Pushpalatha & Byju Gangadharan
Original Article | Published: 18 November 2020 | Pages: 307 - 315

Hydrodynamic modeling of the Utinga source in Belém, Pará, Brazil
Thaís Fonseca de Araújo, Claudio José Cavalcante Blanco ... Yves Secretan
Original Article | Published: 22 October 2020 | Pages: 317 - 329

Formation evaluation of reservoirs in Eocene, Niger Delta Nigeria using modified formation factor from Pickett's plot
Okechukwu E. Agbasi, Magnus U. Igboekwe ... Sunday E. Etuk
Original Article | Published: 21 October 2020 | Pages: 331 - 339

Regionalization of mean annual flow for ungauged catchments in case of Abbay River Basin, Ethiopia
Habtamu Nega & Yilma Seleshi
Original Article | Published: 31 October 2020 | Pages: 341 - 350

Carbon stock potential of Sekele Mariam forest in North Western Ethiopia: an implication for climate change mitigation
Gezahegn Gashu Ewunetie, Birhan Asmame Miheretu & Goitom Tesfaye Mareke
Original Article | Published: 20 November 2020 | Pages: 351 - 362

A multiple regression model to estimate the suspended sediment yield in Italian Apennine rivers by means of geomorphometric parameters
Sergio Grauso, Francesco Pasanisi ... Marcello Grillini
Original Article | Published: 18 January 2021 | Pages: 363 - 371

Statistical comparison between the standardized precipitation index and the standardized precipitation drought index
Nabil Mega & Abderrahmane Medjerab
Original Article | Published: 15 January 2021 | Pages: 373 - 388

Hydrochemistry and quality assessment of qanat water compared to wells using laboratory studies and literature review (case study of Samalghan plain, North Khorasan, Iran)
Abdulmannan Rouhani
Original Article | Published: 02 November 2020 | Pages: 389 - 401

Geohazard characterization of subsurface materials using integrated geophysical methods for post foundation studies: a case study
Akindeji O. Fajana
Original Article | Published: 18 June 2020 | Pages: 403 - 415

Impact of coupling terms on the thermal transport mechanism in a fracture matrix coupled system
N. Natarajan, G. Suresh Kumar & M. Vasudevan
Original Article | Published: 30 June 2020 | Pages: 417 - 432

Modeling infiltration in surface irrigation with minimum measurement (study of USDA–NRCS intake families)
Mohammad Mahdi Chari, Mohammad Taher Poozan & Peyman Afrasiab
Original Article | Published: 28 June 2020 | Pages: 433 - 441

Modeling predictive suitability to determine potential areas for establishing wind power plants in Sri Lanka
A. G. Amarasinghe & E. N. C. Perera
Original Article | Published: 13 July 2020 | Pages: 443 - 454

Modeling of the PM_{10} pollutant health effects in a semi-arid area: a case study in Zabol, Iran
Safoura Javan, Somayeh Rahdar ... Mahmoud Taghavi
Original Article | Published: 14 July 2020 | Pages: 455 - 463

Assessment and comparison of Digital Elevation Model (DEM) products in varying topographic, land cover regions and its attribute: a case study in Shikoku Island Japan
Kwanchai Pakoksung & Masataka Takagi
Original Article | Published: 18 July 2020 | Pages: 465 - 484

Medium-term forecasts for salinity rates and groundwater levels
Ihsan A. Abuamra, Ashraf Y. A. Maghari & Hussam F. Abushawish
Original Article | Published: 25 July 2020 | Pages: 485 - 494

Modeling of reference evapotranspiration for temperate Kashmir Valley using linear regression
Syed Mohsin & M. A. Lone
Original Article | Published: 07 August 2020 | Pages: 495 - 502

Spatio–temporal rainfall trend anomalies in Vidarbha region using historic and predicted data: a case study
Saranya C. Nair & Ashwini B. Mirajkar
Original Article | Published: 18 August 2020 | Pages: 503 - 510

Solar-powered pump drip irrigation system modeling for establishing resilience livelihoods in South Omo zone and Afar regional state, Ethiopia
Mamuye Tebebal Ejigu
Original Article | Published: 10 August 2020 | Pages: 511 - 521

Trend analysis of reference evapotranspiration and identification of responsible factors in the Jhelum River Basin, Western Himalayas
Syed Mohsin & M. A. Lone
Original Article | Published: 23 July 2020 | Pages: 523 - 535

Color slices analysis of land use changes due to urbanization in a city environment of Miami Area, South Florida, USA
Y. Divya, P. Gopinathan ... Ayad M. Fadhil Al-Quraishi
Original Article | Published: 16 July 2020 | Pages: 537 - 546

Infiltration in vegetated soil: empirical modeling and sensitivity analysis
Md. Enayet Chowdhury, Mohammad Shariful Islam ... Humaira Anisa
Original Article | Published: 04 July 2020 | Pages: 547 - 559

A statistical method for analysing temperature increase from remote sensing data with application to Spitsbergen Island
Cendana Fitrahanjani, Tofan Agung Eka Prasetya & Rachmah Indawati
Original Article | Published: 01 August 2020 | Pages: 561 - 569

GIS and multi-criteria decision-making assessment of sites suitability for agriculture in an anabranching site of sooin river, India
Sunil Saha, Debabrata Sarkar ... Sanjit Goswami
Original Article | Published: 09 August 2020 | Pages: 571 - 588

Quantification of flood mitigation services by urban green spaces using InVEST model: a case study of Hyderabad city, India
Ashok Kadaverugu, Ch Nageshwar Rao & G. K. Viswanadh
Original Article | Published: 12 August 2020 | Pages: 589 - 602

Performance and estimation of solar radiation models in state of Minas Gerais, Brazil
Angélica Carvalho Cunha, Luís Roberto Almeida Gabriel Filho ... Fernando Ferrari Putti
Original Article | Published: 16 September 2020 | Pages: 603 - 622

Impact of population density on Covid-19 infected and mortality rate in India
Arunava Bhadra, Arindam Mukherjee & Kabita Sarkar
Short Communication | Published: 14 October 2020 | Pages: 623 - 629

Predicting modeling scenarios of climate change impact on the CO_2 emissions from an Amazonian hydroelectric reservoir
Marcelo Curtarelli, José Stech ... Igor Ogashawara
Short Communication | Published: 09 August 2020 | Pages: 631 - 639

← Previous | 1 | 2 | Next →

Modeling Earth Systems and Environment (2021) 7:561–569
https://doi.org/10.1007/s40808-020-00907-6

ORIGINAL ARTICLE

A statistical method for analysing temperature increase from remote sensing data with application to Spitsbergen Island

Cendana Fitrahanjani[1] · **Tofan Agung Eka Prasetya**[2] · **Rachmah Indawati**[1]

Received: 16 April 2020 / Accepted: 25 July 2020 / Published online: 1 August 2020

Abstract

Arctic plays as a key climatic region, it is highly affected by climate change. Climate change has long been considered as an effect of global warming, it is derived from complex linkages and changes in climate variables. Land surface temperature (LST) is known as one of the essential climate variables (ECVs). Recent study founds that LST has risen in the Arctic. Due to the rising temperatures, there has been a massive decrease in basic Arctic features, which elevated the percentage of heat trapped in the surface. LST is an ECV which needs to be further investigated in key regions. This study aims to investigate LST changes over February 2000 to November 2019 in Spitsbergen. We used autoregression and multivariate regression with cubic spline used to investigate LST changes over this period in Spitsbergen. Four knots and seven knots cubic spline were applied, respectively, to detect acceleration and 7-year cycle. Research founds that LST in Spitsbergen rise by 1.039 °C per decade (CI 0.576–1.501; z: 4.403). Gustav Adolf Land, Nordaustlandet has the highest temperature rise, location of the well-known Vegafonna ice-caps. A notable increase has shown during winter days.

Keywords Land surface temperature · Spitsbergen · Arctic · Climate change

Introduction

Since the first World Climate Conference (in Geneva 1979) scientists have recognized the urgency of the climate change problem. It was leading to the establishment of the World Climate Program, as an effort to develop technology and collect information related to climate change and variation. In the meantime, the global climate observing system (GCOS) has determined essential climate variables (ECVs) which used to describe climate change. It is necessary to evaluate these variables to give us a better understanding of climate change and how severe it has affected our World.

To date, there have been numerous tools to facilitate the need of evaluating ECVs. For instance, the National Aeronautics and Space Administration (NASA) has launched hundred satellite remote sensors and most of them are used to observed ECVs. One of the known ECVs is the land surface temperature (LST). LST is a basic climate change parameter and a manifestation of energy exchanges between the atmosphere and biosphere (Malamiri et al. 2018; Mutiibwa et al. 2015; Williamson et al. 2014). LST in the Arctic region has risen twice as rapidly as global temperature (Muster et al. 2015). Warming LST causing land surface properties to disturbed, especially in areas underlain by permafrost (Muster et al. 2015). This region is vulnerable to climate change, so Arctic designated as a key region in the global climate system (Zhou et al. 2014). In a permafrost environment, LST plays a vital role to provide information in understanding glacier components (Shukla and Dar 2015) and becomes an important parameter for the energy budget (Li et al. 2019). However, there are large discrepancies in climate models in the Arctic, which leads to an even larger uncertainty than at lower latitudes area (Adakudlu et al. 2019). Then, analyze LST in Spitsbergen would be needed to achieve a useful knowledge base for understanding climate change in this area (Adakudlu et al. 2019). Several studies have also carried out various statistical modeling to analyze LST. They estimate LST trends using weighted least squares (Wongsai et al. 2017), ordinary least square regression (Muro et al. 2018), linear regression (Firoozi et al. 2020; Me-Ead and

✉ Cendana Fitrahanjani
cendana.fitrahanjani-2016@fkm.unair.ac.id

1 Biostatistics and Demography Department, Public Health Faculty, Universitas Airlangga, Surabaya, Indonesia

2 Health Department, Faculty of Vocational Studies, Universitas Airlangga, Surabaya, Indonesia

McNeil 2019), Mann–Kendall (Zhao et al. 2019), multivariate adaptive regression splines (Mustafa et al. 2020), and cubic spline regression and generalized estimated equation (Suwanwong and Kongchouy 2016).

LST is remotely-sensed data. The remote sensor covers a large area and accounts for multi-source, multi-variable, and multi-scale data with different spatial and temporal attributes (Guo et al. 2015). This has become a challenge due to missing data or errors because of the high uncertainty involved in data acquisition. Missing data in analysis can interfere with the result, makes the prediction of the observed value becomes inaccurate. Therefore, there must be an appropriate selection due to the statistical analysis model. It is required to impute all missing values before further analyses conducted. Cubic spline function are simple and well-known which are often fitted for regression analysis (Perperoglou et al. 2019) and modeled to handle missing data (Me-Ead and McNeil 2019). The use of cubic spline is considered as giving a high accuracy to estimate missing value. Restricted cubic spline to knots number and placement is subject to the user, which are useful to make a continuous and smooth prediction (Gauthier et al. 2020). In this work, we would like to present seasonal patterns of LST in Spitsbergen by plotting the LST average value, also present LST changes in Spitsbergen using the autoregression and multivariate regression with cubic spline. The results are useful to provide evidence of warming LST trends in Spitsbergen as an effect of climate change, also provide statistical methods that can be used to model LST.

Methods

Study area

The study area is Spitsbergen of the Svalbard Archipelago (see Fig. 1). It is at 74°–81° north and 10°–35° east. Svalbard's climate is mild as a result of its location between two oceanic currents. Both west and east oceanic currents affect sea surface temperature and sea ice distribution. Along the west coast, climate in Svalbard is subpolar while the east coast has freezing temperatures even during summer. Winter is longer and occurs from August to May while summer occurs from June to August. Svalbard has unique features because it is located in the Arctic region. Svalbard is a glaciated area (60%). Glaciation increases generally with altitude and to the west. Edgeøya, Barentsøya, and Nordaustlandet are the most extensive glaciated area. The northern area brings a lot of snow marked by wide ice caps. Among the Arctic region, Spitsbergen has the warmest permafrost with mean air temperatures ranging from about − 2.5 °C at coastal western sites to − 5 °C in central parts (Adakudlu et al. 2019).

Data source

This study used moderate resolution imaging spectroradiometer (MODIS) Terra NASA Satellite product. Terra satellite orbits from north to south of the Earth and observes LST in the morning. The MODIS Terra Satellite product used in this study is the MOD11A2 8-day LST, an LST data per 8-day period. The recorded data will be processed

Fig. 1 Location of study area (Source: Google Earth, 2020)

by Land Active Distributed Archive Center (LP DAAC) which responsible as a data processor, storage, and distributor to users. Users were expected to register an account to be able to use the data. Accounts that had been registered with NASA's Earth data had access to download the data set. Data was then sent via email. In this article, we analyzed LST changes using data from February 2000 to November 2019. LST is in kelvin, we convert it to celcius.

Sample selection

Considering the concept of sampling in a statistical method, for this study nine sub-regions were designed to represent the entire Spitsbergen. Nine sub-regions were used on consideration of one region representative and measure to avoid spatial correlation. The determination of the sample point started from the uppermost of the region based on its longitude and latitude. The next point was determined by converting coordinate in vertical tiles, horizontal tiles, lines, and samples with the help of the Modland tile calculator tool. The sample point determination must be precise and are not in water territorial. Figure 2 shows each sample point, hereby the sub-regions, to investigate LST changes in Spitsbergen. Terra Satellite uses a spatial resolution of 1×1 km^2. For each sub-regions, we use the smallest area of 7×7 km^2 to get detailed information about daytime LST.

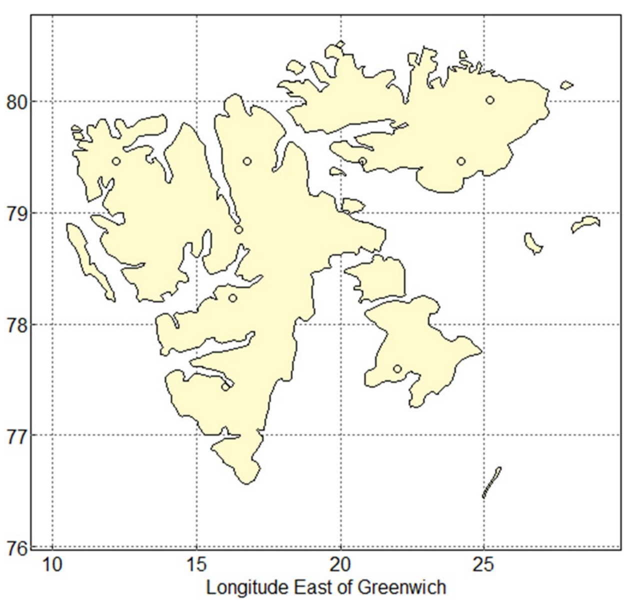

Fig. 2 Spitsbergen sub-regions. Each bullet represents sub-region as sample point

Data analysis

Seasonal pattern

A seasonal pattern is used to determine temperature variations. With seasonal patterns, we know when the temperature will rise or fall affected by the time of the year, simply because the value is influenced by the value at the same time of the previous year. An autoregression model implies that a value is influenced by value in the past time. Observation of the value that is at a lag order shows the extent to which the dependency level of the observed value is influenced by a value at a past time which are useful to make predictions (Brockwell and Davis 2002).

Seasonal patterns for each sub-region are shown in Fig. 3 by plotting daytime LST average values per day each year. We assumed a constant seasonal pattern for each sub-region because data derived from a satellite is a highly temporal, which causes the data to vary greatly and fluctuate during the observation time. A natural cubic spline is used to ensure a smooth and continuous seasonal pattern between years. The use of natural cubic spline is inseparable from its parameter known as knots, where the number of knots and their placement determine a smooth and continuous seasonal pattern (Gauthier et al. 2020). In this article, we use eight knots. The location of the knots used is considered a "best practice" for analyzing LST data located on Julian Days 10, 35, 60, 90, 115, 310, 335, and 355 (Wongsai et al. 2017).

Time series correlation models

After the autoregression model identified a seasonal pattern, the spline-smoothed seasonal pattern as a seasonal component is substracted to make a seasonal adjustment (Brockwell and Davis 2002). Constant added to preserve overall means to provide a stationary time series. To remove the autocorrelation effect, the data were filtered using the second-order autoregressive [AR(2)] model (equivalent to 8-day LST data). Then we fitted the temperature data using multivariate regression with cubic spline.

Adjusting for spatial correlation

To adjust spatial correlation, we used multivariate regression because this model is commonly used to analyzed any number of response variables that have the same predictor variables with mutually correlated errors. This model also uses a matrix response to create a confidence interval (Mardia et al. 1979).

LST retrieval is dealt with the occurrence of missing data. Missing data resulted from Terra Satellite limitations to observes on cloudy days (Mutiibwa et al. 2015) and/or water vapor (Me-Ead and McNeil 2019). Cloudiness influenced the

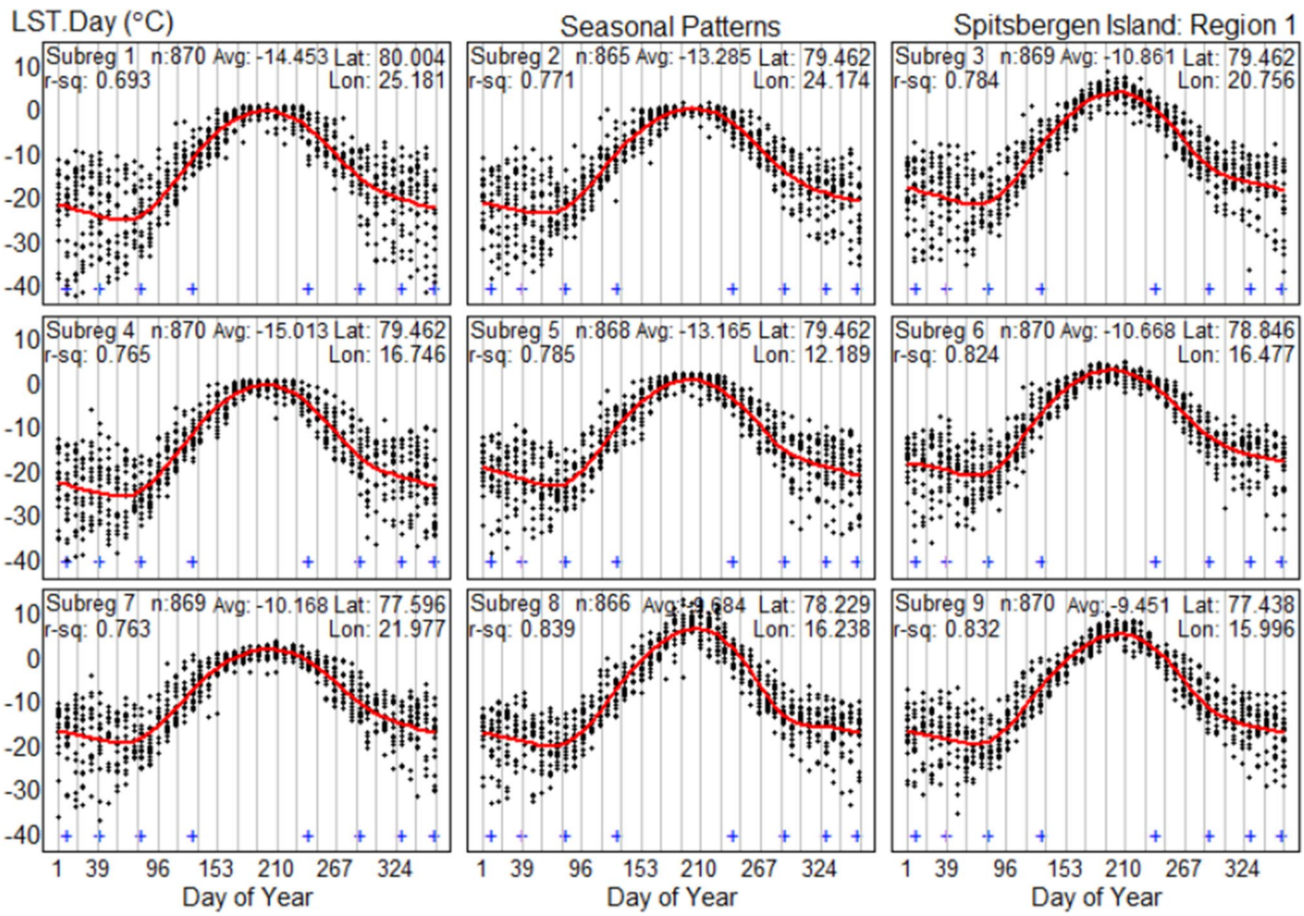

Fig. 3 Spitsbergen seasonal pattern. Horizontal axis is day of year (1–365) while vertical axis is daytime LST in °C. The "Lat and Lon" label displays sub-region ordinate. The "Avg" label indicates mean annual LST in each sub-region. The "n" label indicates observation number. Eight blue plus indicates "best practice" knots located on Julian days 10, 35, 60, 90, 115, 310, 335 and 355. The black dots is LST per day each year. Red curve is smooth-seasonal pattern from LST average per day each year

quality of LST products (Kenawy and Hereher 2019) resulting in sensor errors in data retrieval (Malamiri et al. 2018). In the Arctic, missing data are likely to occur and somehow unavoidable. Arctic is an area with a high annual cloud cover (He et al. 2019; Shupe 2011). Missing data is estimated with spline models.

We fitted straight line models to estimate linear trends, whereas cubic splines fitted to detect acceleration and cycle that might be present. Four knots used to estimate acceleration (knots located on the year 2000, 2006, 2012, and 2018). Seven knots used to detect whether a 7-year cyclic pattern is likely to appear (knots located in the year of 2000, 2003, 2006, 2009, 2012, 2015, dan 2018).

Results and discussion

Snow and ice are sensitive indicators of climate change. It is sensitive with a slight change in temperature and causes the heating and thawing of freezing ground (permafrost) and glaciers in the Arctic (Song et al. 2018). Although Antarctic also covered with ice and has the same natural properties as the Arctic, as opposed to the Arctic, Antarctic experienced a cooling trend. Ice in the Arctic behaves differently than Antarctic's. Ice loss in the Arctic releases more heat to space (Rudels 2016). Thus, scientists took Arctic as concerned to studied climate change variables.

Greater ice loss will affect the extent of the dark open water area which will absorb heat from the sun. These will further results to even more ice loss and affects other climate variables. The more heat absorbed, the more permafrost begins to thaw, microorganisms start to break down organic matter in the soil and released carbon dioxide (CO_2), methane (CH_4) and nitrous oxide (N_2O) into the air and accelerate global warming (Turetsky et al. 2019). When an object has no balance in the mechanism of receiving and releasing energy, it responds with an increase or decrease in temperature. For example, if 71% of the energy is absorbed by the Earth's surface, so the same amount is needed to keep the temperature stable. In terms of land surface energy budget, LST is the appropriate measurement used to describe this condition (Crago and Qualls 2014).

In Fig. 3, we display a seasonal pattern by plotting the average LST each day of the observation period (February 2000–November 2019) in nine sub-regions. Our study founds that based on the seasonal pattern, in winter days, LST in Spitsbergen experienced a warming trend. This can be seen from a scattered value in the plot compared to summer days (June–August). Started from early March (day 60), LST rises gradually until it reaches maximum temperature in July. July is the warmest month of the year. Førland, et.al. (2011) who studied the temperature changes, founds that the warming trend occurs mainly during winter and spring in Svalbard. Isaksen et al. (2016) also found that warming in Spitsbergen mainly occurs in winter. During winter, temperature increased by 2–3 °C per decade. Although winter is the longest season, there has been shortening in the winter period, a response to the rising temperature. Rising winter temperature is an important aspect of climate change. It is associated with atmospheric circulation, air mass characteristics, and sea ice concentration. According to Cohen et al. (2018), warm Arctic can lead to more frequent severe winter weather in other regions in the world.

There are 46 observations in a year for 8-day LST. During February 2000–November 2019 there are 875 observations. In this study, there is an indication of missing data during the observation period ("n" indicates number of observation below the maximum observation in a year). Remotely sensed data suffer from cloud contamination (Metz et al. 2017) and likely leads to the occurrence of missing data. Cloud-cover inhibits LST retrieval. Cloud cover is a component in the climate system and its frequency is related to the radiation budget, especially in the key climate region. Areas that are highly affected by climate change, like the Arctic, have a higher cloud-cover than other regions. Briefly, this happens because of the energy exchange between surface and atmosphere, sea-ice retreats which further doubled evaporation over the melted area. Evaporation in an area will increase cloud-cover. Higher evaporation makes cloud-cover to extend. In Spitsbergen, cloud-cover is more frequent in summer than in winter days (Cisek et al. 2017; Maturilli and Ebell 2018). Serreze and Barry (2014) mentioned that the cloud-cover in Spitsbergen is ranging from 60% in winter and 80% in August and September. Consequently, missing data is unavoidable in this region. It is seen that there are more missing data found in sub-region 8, Longyearbyen. There are only 866 observations available during the period being observed. Further study should be conducted to improve the cloud detection algorithm (Li et al. 2019), especially in the Arctic.

Missing data are handled with a natural cubic spline function. A cubic spline is a function that connects two points. A smooth curve can be generated if fitted at points with a certain number and interval, known as "knots". Cubis spline is flexible and there is no limitation in knots determination. According to Perperoglou et al. (2019), knots number and placement are determined by the user where the number and locations are unique for one data set to another. Daily or monthly LST data might not follow the same knot number and placement, it is suggested for users to determine the "best practice" knots number which ensures smooth periodicity. Make sure the chosen knots number and locations are not "overfitting", i.e. the spline function is too close to the observation value and fails to estimate missing data. Overfitted commonly occurs when users considered using too large knots. Figure 3 demonstrates how cubic spline function can be used to ensure a continuous and smooth seasonal pattern using eight knots at the "best practice" location (Julian days 10, 35, 60, 90, 115, 310, 335 and 355) and perform a good estimation for missing values, with high r-squared.

Figure 4 displays a seasonal adjustment time series. According to Brockwell and Davis (2002), season-adjusted time series is a procedure to subtract seasonal components in time series. In this work, a smooth-seasonal pattern is subtracted to remove the seasonal components and obtain a stationary model. We added constant to preserve overall mean, so the model has a constant mean at every time points. Box et al. (2016) have mentioned that a stationary time series is one with constant mean, variance, and autocorrelation over time, it doesn't change over time. A stationary time series is a data series without a trend component or seasonal components. Most of the time series models are needed to satisfied a stationary assumption and useful for forecasting. An autoregressive model implies that a data (y_t) is influenced by data in previous time (y_{t-1}, y_{t-2}, y_{t-3}, …), called autocorrelation. Then, it is required to found an autocorrelation effect for LST data. After founding the autocorrelation, one would be needed to remove the autocorrelation effect before fitted with a regression model. Then a completed and uncorrelated error can be used to investigate LST changes using multivariate regression. Multivariate regression analyses provide an LST increase per decade in each sub-region and

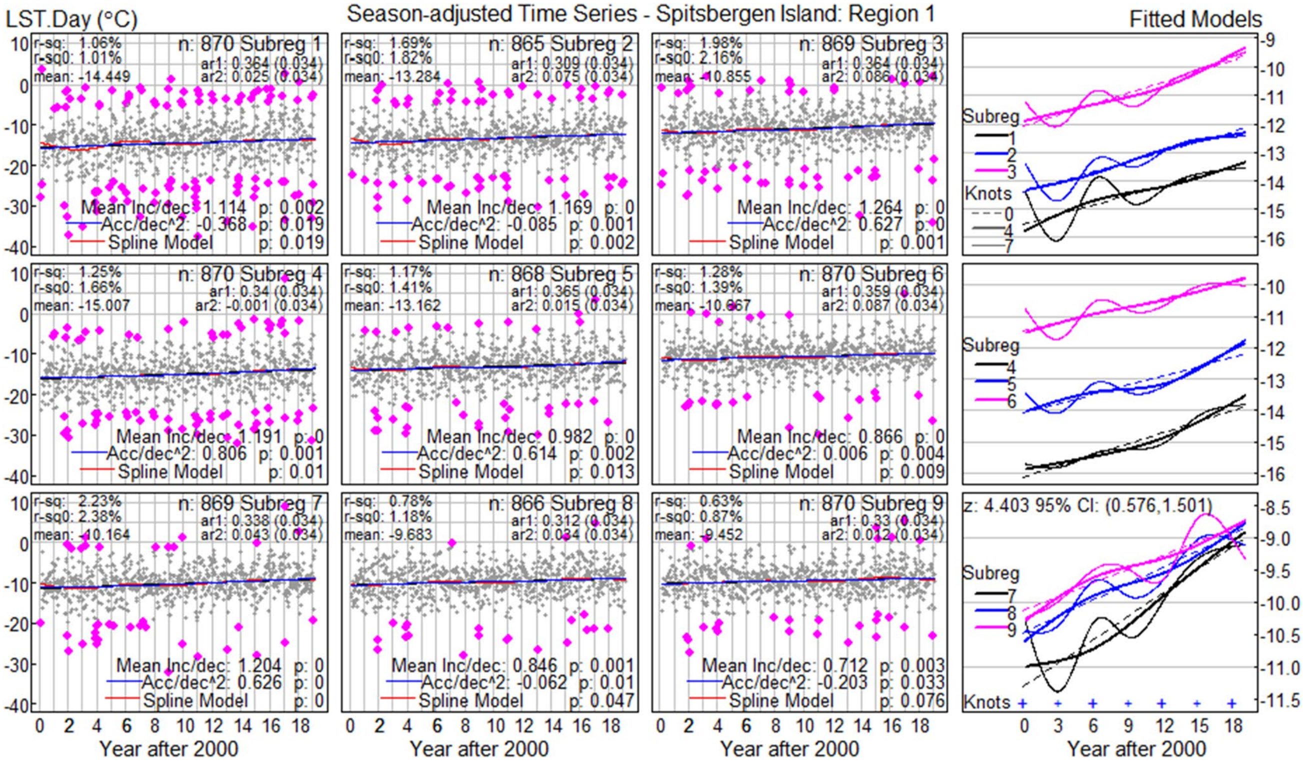

Fig. 4 Season-adjusted time series

Table 1 Mean increased LST for each sub-regions

	Latitute	Longitude	Mean Inc/dec[a] (°C)	Acc/dec2[b] (°C)	AR (1)[c]	SE 1[d]	AR (2)[e]	SE 2[f]
Sub-region								
1	80.004	25.181	1.114	−0.368	0.364	0.034	0.025	0.034
2	79.462	24.174	1.169	−0.085	0.309	0.034	0.075	0.034
3	79.462	20.756	1.264	0.627	0.364	0.034	0.086	0.034
4	79.462	16.746	1.191	0.806	0.340	0.034	−0.001	0.034
5	79.462	12.189	0.982	0.614	0.365	0.034	0.015	0.034
6	78.846	16.477	0.866	0.006	0.359	0.034	0.087	0.034
7	77.596	21.977	1.204	0.626	0.338	0.034	0.043	0.034
8	78.229	16.238	0.846	−0.062	0.312	0.034	0.034	0.034
9	77.438	15.996	0.712	−0.203	0.330	0.034	0.012	0.034
Region								
Spitsbergen			Mean Inc/dec: 1.039 °C; CI (0.576–1.501); *z*: 4.403					

[a]Mean increase in each sub-region/region per decade

[b]Acceleration in each sub-region per decade

[c]First-order autoregressive constant

[d]First-order autoregressive standard error

[e]Second-order autoregressive constant

[f]Second-order autoregressive standard error

Spitsbergen. Outliers (the pink dots in Fig. 4) remove in this study to provide a normally distributed data.

LST is risen in each sub-region (see Table 1). The highest temperature rise occurred in sub-region 3 for Gustav Adolf Land, the location of Vegafonna ice-cap on Nordaustlandet Island (1.264 °C per decade). Besides, temperature in sub-region 1 and 2 (located on Nordaustlandet Island) increased 1.114 °C dan 1.169 °C per decade. Nordaustlandet Island is mostly covered with ice-cap; Austfonna, Vestfonna, and Vegafonna. Austfonna covers most of Nordaustlandet areas. Ice-cap is one form of glaciers, which is highly sensitive to climate change (Qin and Ding 2010). Glacier forms from a long-term snow deposition on the land. Glaciers' changes affect land temperature. The warmth land temperature can be explained by the interaction between changes cryosphere and biosphere components (Qin et al. 2018), also other Earth's spheres. Each component will respond differently to climate change and lead to temperature increased.

To investigate LST in Spitsbergen, we used multivariate regression with cubic spline. Unlike the use of natural cubic spline for seasonal pattern, cubic spline fitted in multivariate regression places knots in certain years for different purposes. We used four-knots cubic spline (located in the year of 2000, 2006, 2012, dan 2018) to estimate temperature acceleration and seven-knots (located on the year of 2000, 2003, 2006, 2009, 2012, 2015, dan 2018) to detect a 7-year cycle. Table 1 displays whether LST in each sub-region has a negative or positive acceleration. Acceleration is used to describe whether temperature rapidly or slowly increase. Sub-region 3, 4, 5, 6, and 9 have positive acceleration, the rest have negative accelaration. Sub-region with positive acceleration experienced rapid increase per decade. LST increased in Spitsbergen is cyclical as illustrated by the cubic spline curve. We can infer that the temperature at Spitsbergen has been decreased at certain times.

To our knowledge, there is no research studied LST in Spitsbergen or Svalbard archipelago. But we found some research which analyzed LST in the Arctic and sub-Arctic (Li and Shiklomanov 2015; Pepin et al. 2019; Sobrino et al. 2020; Westergaard-Nielsen et al. 2018). They have mentioned that the Arctic region is warming. Most studies analyzed air temperature than LST such as (Førland et al. 2011; Nordli et al. 2014; Piskozub 2017). They have agreed that there has been air temperature increased in the Arctic three times higher than the estimated increase in global warming. However, Førland et al. (2011) found that there has been a cooling trend in Svalbard during 1943–1965, then starts to increase again from the mid-1960s (Nordli et al. 2014). Both air temperature and LST can be used as a measurement to explain surface-atmosphere interactions and energy fluxes between the atmosphere and the ground (Zhang et al. 2015) and designated as key variables to climate change. Compared to air temperature, LST has a warmer value during summer days and colder during winter days because air temperature and LST are based on different physical meanings and different responses to atmospheric conditions (Mutiibwa et al. 2015). If we associate LST with several key climatic and environmental variables, it could have a high correlation with air temperature (Kenawy and Hereher 2019). Hooker et al. (2018) have developed a dataset, where air temperature can be predicted from monthly LST. However, LST is a better parameter than air temperature to explain energy budget in the Arctic, sub-Arctic and alpine environment (Williamson et al. 2014).

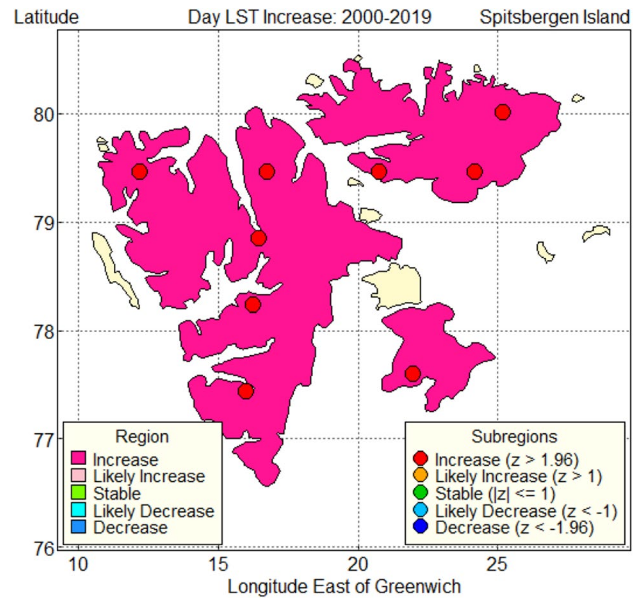

Fig. 5 Day LST increase (2000–2019)

Spitsbergen temperature has risen 1.039 °C per decade (Table 1). In Fig. 5, we have presented a picture to describe our investigation in Spitsbergen. We set a boundaries with normal distribution (z) to determine whether LST in sub-region or region is increase ($z > 1.96$), likely increase ($z > 1$), stable ($|z| \leq 1$), likely decrease ($z < -1$), or decrease ($z < -1.96$). Figure 5 displays LST Spitsbergen has increased (z: 4.403).

Arctic acts as World's refrigerator. A substantial change in the Arctic due to climate changes will result in a higher amount of heat stored by Earth's surface and affecting other regions in the World. LST increased in the Arctic, but not necessarily increased in other regions. According to Song et al. 2018, LST has increased across 62.4% of the land area in the world, the rest has decreased. Climate change is a serious problem and might take as a deep concern. It is not only responsible for the emergence of extreme natural disasters, drought, or crop failures but also threatening human health.

Conclusion

In this paper, we apply simple and well-known analyses to investigate LST changes in Spitsbergen, using autoregression and multivariate regression with cubic spline. These two statistical models are used because remotely-sensed data is obtained continuously in a long period and covers a large area which makes LST is a spatial data. With the autoregression model, we found that the autocorrelation effect for 8-day LST is at the second lag and then filtered to ensure the data can be used for multivariate regression. The natural cubic spline has long been considered as a very useful model to ensure a smooth and continuous periodicity. The use of eight-knots number and placement for 8-day LST has proven that smooth periodicity (high r-squared) is obtained, so that missing data can be resolved. Outliers removed from multivariate regression to ensure a good analysis. Our research found that LST in Spitsbergen is increased by 1.039 °C per decade (CI 0.576–1.501; *z*: 4.403). Although July has the maximum temperature, the most notable LST changes occurred in winter days. Gustav Adolf Land, Nordaustlandet, has the highest temperature increased per decade (1.264 °C).

Acknowledgements We thank Prof. Don McNeil (Prince of Songkla University Thailand) who assisted with methodology, developed, and tested the R software.

Author contributions CF analyzed the data and wrote this manuscript. TAEP designed sample point, revise and update R syntax. RI helping with the manuscript drafting. All authors read and approved the final manuscript.

Funding Not applicable.

Data availability The MODIS 8 days Terra LST (MOD11A22) data that support the findings of this study are available in Global Subsets Tool: MODIS/VIIRS Land Products [hyperlink to datasets source "https://modis.ornl.gov"].

Code availability The data is analyzed by open source software: R version 3.6.1. Code unavailable.

Compliance with ethical standards

Conflict of interest The authors declare that they have no conflict of interest.

References

Adakudlu M, Andersen J, Bakke J, Beldring S, Benestad R, Bilt W, Bogen J, Borstad C, Breili K, Breivik Ø, Børsheim KY, Christiansen HH, Dobler A, Engeset R, Frauenfelder R, Gerland S, Gjelten HM, Gundersen J, Isaksen K, Jaedicke C, Kierulf H, Kohler J, Li H, Lutz J, Melvold K, Mezghani A, Nilsen F, Nilsen J, Pavlova O, Ravndal O, Risebrobakken B, Saloranta T, Sandven S, Schuler TV, Simpson M, Skogen M, Smedsrud LH, Sund M, Vikamar-Schuler D, Westermann S, Wong WK (2019). Climate in Svalbard 2100. Report. ISSN: 2387-3027

Box GEP, Jenkins GM, Reinsel GC, Ljung GM (2016) Time series analysis, 5th edn. John Wiley & Sons, New Jersey

Brockwell PJ, Davis RA (2002) Introduction to time series and forecasting, 2nd edn. Springer, New York

Cisek M, Makuch P, Petelski T (2017) Comparison of meteorological conditions in Svalbard fjords: Hornsund and Kongsfjorden. Oceanologia 59(4):413–421. https://doi.org/10.1016/j.oceano.2017.06.004

Cohen J, Pfeiffer K, Francis JA (2018) Warm Arctic episodes linked with increased frequency of extreme winter weather in the United States. Nature Commun 9(1):1–12. https://doi.org/10.1038/s41467-018-02992-9

Crago RD, Qualls RJ (2014) Use of land surface temperature to estimate surface energy fluxes: contributions of Wilfried Brutsaert and collaborators. Water Resour 50:3396–3408. https://doi.org/10.1002/2013WR015223.Received

Firoozi F, Mahmoudi P, Jahanshahi SMA, Tavousi T, Liu Y, Liang Z (2020) Modeling changes trend of time series of land surface temperature (LST) using satellite remote sensing productions (case study: Sistan plain in east of Iran). Arab J Geosci 13(10):1–14. https://doi.org/10.1007/s12517-020-05314-w

Førland EJ, Benestad R, Hanssen-Bauer I, Haugen JE, Skaugen TE (2011) Temperature and precipitation development at Svalbard 1900–2100. Adv Meteorol 2011:1–14. https://doi.org/10.1155/2011/893790

Gauthier J, Wu QV, Gooley TA (2020) Cubic splines to model relationships between continuous variables and outcomes: a guide for clinicians. Bone Marrow Transplant 55:675–680. https://doi.org/10.1038/s41409-019-0679-x

Guo HD, Zhang L, Zhu LW (2015) Earth observation big data for climate change research. Adv Clim Change Res 6:108–117. https://doi.org/10.1016/j.accre.2015.09.007

He M, Hu Y, Chen N, Wang D, Huang J, Stamnes K (2019) High cloud coverage over melted areas dominates the impact of clouds on the albedo feedback in the Arctic. Sci Rep 9:1–11. https://doi.org/10.1038/s41598-019-44155-w

Hooker J, Duveiller G, Cescatti A (2018) Data descriptor: a global dataset of air temperature derived from satellite remote sensing and weather stations. Sci Data. https://doi.org/10.1038/sdata.2018.246

Isaksen K, Nordli Ø, Førland EJ, Łupikasza E, Eastwood S, Niedźwiedź T (2016) Influence of atmospheric circulation and sea ice cover. J Geophys Res Atmos 121:11913–11931. https://doi.org/10.1002/2015JD023134

Kenawy AMEl, Hereher ME (2019) An assessment of the accuracy of MODIS land surface temperature over egypt using ground-based measurements. Remote Sens 11:1–29

Li Z, Shiklomanov NI (2015) Impacts of urban and industrial development on Arctic land surface temperature in Lower Yenisei River Region. AGU Fall Meeting Abstracts 2015:GC31B–1182

Li A, Xia C, Bao C, Yin G (2019) Using MODIS land surface temperatures for permafrost thermal modeling in beiluhe basin on the Qinghai-Tibet plateau. Sensors. https://doi.org/10.3390/s19194200

Malamiri HRG, Rousta I, Olafsson H, Zare H, Zhang H (2018) Gap-filling of MODIS time series land surface temperature (LST) products using singular spectrum analysis (SSA). Atmosphere. https://doi.org/10.3390/atmos9090334

Mardia KV, Kent JT, Bibby JM (1979) Multivariate analysis. Academic Press, San Diego

Maturilli M, Ebell K (2018) Twenty-five years of cloud base height measurements by ceilometer in Ny-Ålesund, Svalbard.

Earth Syst Sci Data 10:1451–1456. https://doi.org/10.5194/essd-10-1451-2018
Me-Ead C, McNeil R (2019) Pattern and trend of night land surface temperature in Africa. Sci Rep 9:18302. https://doi.org/10.1038/s41598-019-54703-z
Metz M, Andreo V, Neteler M (2017) A new fully gap-free time series of land surface temperature from MODIS LST data. Remote Sens 9:1333. https://doi.org/10.3390/rs9121333
Muro J, Strauch A, Heinemann S, Steinbach S, Thonfeld F, Waske B, Diekkrüger B (2018) Land surface temperature trends as indicator of land use changes in wetlands. Int J Appl Earth Obs Geoinf 70:62–71. https://doi.org/10.1016/j.jag.2018.02.002
Mustafa EK, Co Y, Liu G, Kaloop MR, Beshr AA, Zarzoura F, Sadek M (2020) Study for predicting land surface temperature (LST) using landsat data: a comparison of four algorithms. Adv Civ Eng 2020:1–16
Muster S, Langer M, Abnizova A, Young KL, Boike J (2015) Spatiotemporal sensitivity of MODIS land surface temperature anomalies indicates high potential for large-scale land cover change detection in Arctic permafrost landscapes. Remote Sens Environ 168:1–12. https://doi.org/10.1016/j.rse.2015.06.017
Mutiibwa D, Strachan S, Albright T (2015) Land surface temperature and surface air temperature in complex terrain. IEEE J Sel Appl Earth Obs Remote Sens 8:4762–4774. https://doi.org/10.1109/JSTARS.2015.2468594
Nordli Ø, Przybylak R, Ogilvie AEJ, Isaksen K (2014) Long-term temperature trends and variability on spitsbergen: the extended svalbard airport temperature series, 1898–2012. Polar Res 33:1–48. https://doi.org/10.3402/polar.v33.21349
Pepin NC, Pike G, Read S, Williams R (2019) The ability of moderate resolution imaging spectroradiometer land surface temperatures to simulate cold air drainage and microclimates in complex Arctic terrain. Int J Climatol 39:953–973. https://doi.org/10.1002/joc.5854
Perperoglou A, Sauerbrei W, Abrahamowicz M, Schmid M (2019) A review of spline function procedures in R. BMC Med Res Methodol 19:1–16. https://doi.org/10.1186/s12874-019-0666-3
Piskozub J (2017) Svalbard as a study model of future High Arctic coastal environments in a warming world. Oceanologia 59:612–619. https://doi.org/10.1016/j.oceano.2017.06.005
Qin D, Ding Y (2010) Key issues on cryospheric changes, trends and their impacts. Adv Clim Change Res 1:1–10. https://doi.org/10.3724/SP.J.1248.2010.00001
Qin D, Ding Y, Xiao C, Kang S, Ren J, Yang J, Zhang S (2018) Cryospheric science: research framework and disciplinary system. Natl Sci Rev 5:255–268. https://doi.org/10.1093/nsr/nwx108
Rudels B (2016) Arctic Ocean stability: the effects of local cooling, oceanic heat transport, freshwater input, and sea ice melt with special emphasis on the Nansen Basin. J Geophys Res Oceans 121:4450–4473. https://doi.org/10.1002/2015JC011045
Serreze MC, Barry RG (2014) The Arctic climate system, 2nd edn. Cambridge University Press, New York
Shukla A, Dar I (2015) Influence of varying sensor characteristics on LST estimations in a glacial terrain. Int Geosci Remote Sens Symp 2015:2083–2086. https://doi.org/10.1109/IGARSS.2015.7326212
Shupe MD (2011) Clouds at arctic atmospheric observatories. Part II: thermodynamic phase characteristics. J Appl Meteorol Climatol 50:645–661. https://doi.org/10.1175/2010JAMC2468.1
Sobrino JA, Julien Y, García-Monteiro S (2020) Surface temperature of the planet earth from satellite data. Remote Sens 12:1–6. https://doi.org/10.3390/rs12020218
Song Z, Li R, Qiu R, Liu S et al (2018) Global land surface temperature influenced by vegetation cover and PM 2.5 from 2001 to 2016. Remote Sens 10:1–18. https://doi.org/10.3390/rs10122034
Suwanwong A, Kongchouy N (2016). Cubic spline regression model and gee for land surface temperature trend using modis in the cloud forest of Khao Nan National Park Southern Thailand during 2000–2015. J Eng Appl Sci 11:2387–2395. https://medwelljournals.com/abstract/?doi=jeasci.2016.2387.2395
Turetsky MR, Abbott BW, Jones MC et al (2019) Permafrost collapse is accelerating carbon release. Nature 569:32–34. https://doi.org/10.1038/d41586-019-01313-4
Westergaard-Nielsen A, Karami M, Hansen BU, Westermann S, Elberling B (2018) Contrasting temperature trends across the ice-free part of Greenland. Sci Rep. https://doi.org/10.1038/s41598-018-19992-w
Williamson SN, Hik DS, Gamon JA, Kavanaugh JL, Flowers GE (2014) Estimating temperature fields from MODIS land surface temperature and air temperature observations in a subarctic alpine environment. Remote Sens 6:946–963. https://doi.org/10.3390/rs6020946
Wongsai N, Wongsai S, Huete AR (2017) Annual seasonality extraction using the cubic spline function and decadal trend in temporal daytime MODIS LST data. Remote Sens. https://doi.org/10.3390/rs9121254
Zhang J, Gao S, Chen H, Yu J, Tang Q (2015) Retrieval of the land surface-air temperature difference from high spatial resolution satellite observations over complex surfaces in the Tibetan Plateau. J Geophys Res Atmos 120:8065–8079. https://doi.org/10.1002/2015JD023395
Zhao W, He J, Wu Y, Xiong D, Wen F, Li A (2019) An analysis of land surface temperature trends in the central himalayan region based on MODIS products. Remote Sens 11:1–19. https://doi.org/10.3390/rs11080900
Zhou X, Matthes H, Rinke A et al (2014) Evaluation of Arctic land snow cover characteristics, surface albedo, and temperature during the transition seasons from regional climate model simulations and satellite data. Adv Meteorol 2014:1–15. https://doi.org/10.1155/2014/604157